Supporting Material

"Calcium Transport and Local Pool Regulate Polycystin-2 (TRPP2) Function in Human Syncytiotrophoblast". Cantero MR and Cantiello HF.

Materials and Methods

Human placenta membrane preparation. Apical hST plasma membranes from term human placenta were obtained as previously described (1). Briefly, normal placenta from vaginal deliveries were obtained and immediately processed. The villous tissue was fragmented, washed with ice-cold unbuffered NaCl saline (150 mM), and minced into small pieces. The fragmented tissue was processed, filtered and centrifuged, as previously reported (1). The final pellet was resuspended in a buffer solution containing (in mM): HEPES 10, sucrose 250, and KCl 20, adjusted to pH 7.4, which was aliquoted and stored frozen until the time of the experiment. Apical hST enrichment usually was higher than 26-fold.

Preparation of in vitro translated PC2. In vitro translated PC2 ($PC2_{iv}$) was prepared as previously reported (1). The plasmid pGEM-PKD2 encoding PC2, was *in vitro* transcribed and translated with a reticulocyte lysate system TnT T7 (Promega) by incubation of plasmid DNA (1 μg) and 50 μl of the reaction mixture for 90 min at 30°C. The $PC2_{iv}$ was introduced by dialysis into liposomes as previously reported (1).

Ion channel reconstitution. PC2 containing vesicles were incorporated into lipid bilayers of a reconstitution system. The lipid mixture was a 7:3 ratio of POPC and POPE (20-25 mg/ml, Avanti Polar Lipids, Birmingham, AL) in n-decane. Unless otherwise stated, the *cis* chamber contained a solution of: KCl 150 mM, $CaCl_2$ 10 μM, HEPES 10 mM, at pH 7.40. The *trans* side contained a similar solution with lower KCl (15 mM), to create a KCl chemical gradient. $PC2_{hst}$ was identified as previously reported (1), by a large conductance (~170 pS), K^+-conducting channel, which was inhibited by *trans* (external) amiloride, and *cis* (cytoplasmic side of PC2) anti-PC2 antibody, properties that also ensured its orientation in the reconstituted membrane (1).

Reagents and Ca^{2+} chelation. Unless otherwise stated, reagents were obtained from Sigma-Aldrich (St. Louis, MO). Ethylene-bis(oxyethylenenitrilo)tetraacetic acid (EGTA, 100 mM) was dissolved in NaOH and titrated with HCl to reach pH 7.1 in the stock solution, before use. Ethylenedioxybis(o-phenylenenitrilo)tetraacetic acid (BAPTA, 250 mM) was dissolved in dimethylsulfoxide (DMSO). The concentrated reagents EGTA and BAPTA (16 μl and 8 μl, respectively) were diluted in either *cis* (1600 μl) or *trans* (1000 μl) chambers, buffered at pH 7.4 to reach a final concentration of 1 mM and 2 mM, respectively (see Results). Neither the addition of either chelator, nor vehicle alone to the chamber solution elicited any change in the final pH, which was kept at 7.4 with 10 mM HEPES. Calculations were corroborated by the free on-line site http://www.stanford.edu/~cpatton/CaEGTA-NIST.htm. The final free Ca^{2+} concentration was estimated to be either 0.6 nM or 0.8 nM (pH ~7.4) in the presence of EGTA or BAPTA, respectively. Whenever indicated, $CaCl_2$ was added to the chamber, from stock solutions ranging from 1 mM to 1 M to the final concentrations indicated in the Results section. In all cases, the added Ca^{2+} chelator was kept throughout the entire experiment.

Data acquisition and analysis. Electrical signals were obtained with a PC501A patch clamp amplifier (Warner Instruments, Hamden, CT) with a 10 Gohm feedback resistor. Output (voltage) signals were

low-pass filtered at 700 Hz (3 dB) with an eight pole, Bessel type filter (Frequency Devices, Haverhill, MA). Signals were displayed in an oscilloscope and acquired using pCLAMP 6.0.2. Single channel current tracings were further filtered for display purposes only. Unless otherwise stated, pCLAMP Version 10.0 (Axon Instruments, Foster City, CA) was used for data analysis and Sigmaplot Version 11.0 (Jandel Scientific, Corte Madera, CA) for statistical analysis and graphics. Unless otherwise stated, all tracings shown in this study were obtained at holding potentials between 40 and 60 mV. PC2 channel identification was conducted as previously reported (1). Statistical significance was obtained by unpaired Student's test comparison of sample groups of similar size, and accepted at $p < 0.05$. Average data values were expressed as the mean ± SEM (N) under each condition, where n represents the total number of experiments analyzed.

Results

Diffusional limitation corrections. The 7 to 1 relationship between the $t_{1/2}$ obtained in the presence of 10 μM Ca^{2+} and either EGTA or BAPTA addition, could be explained neither by the binding interaction itself nor by the forward rate constants of the chelators (2). Thus, we explored the possibility that a diffusional limitation of the chelators could exist, limiting their access to Ca^{2+} binding sites. To this end, we corrected the experimental recovery curves by the transport coefficient (h) as described in (3), representing the existence of a diffusional layer between the channel and the bulk Ca^{2+} present, which would have distinct diffusive properties for either chelator. We plotted I_m/I_{max} *vs.* time, after Ca^{2+} addition to the *cis* chamber following inhibition by either EGTA or BAPTA (Fig. S1a), respectively. The h values obtained (Fig. S1b) were not statistically different from each other (see Results Section in the main text, $p > 0.05$), indicating that the two chelators did not display any relevant diffusional differences. The corrected $K_D s$ values obtained (4.70 ± 0.02 nM and 1.26 ± 0.03 nM, in the presence of EGTA and BAPTA addition, respectively) fell within the experimental error, such that the diffusional contribution would be negligible for either chelator.

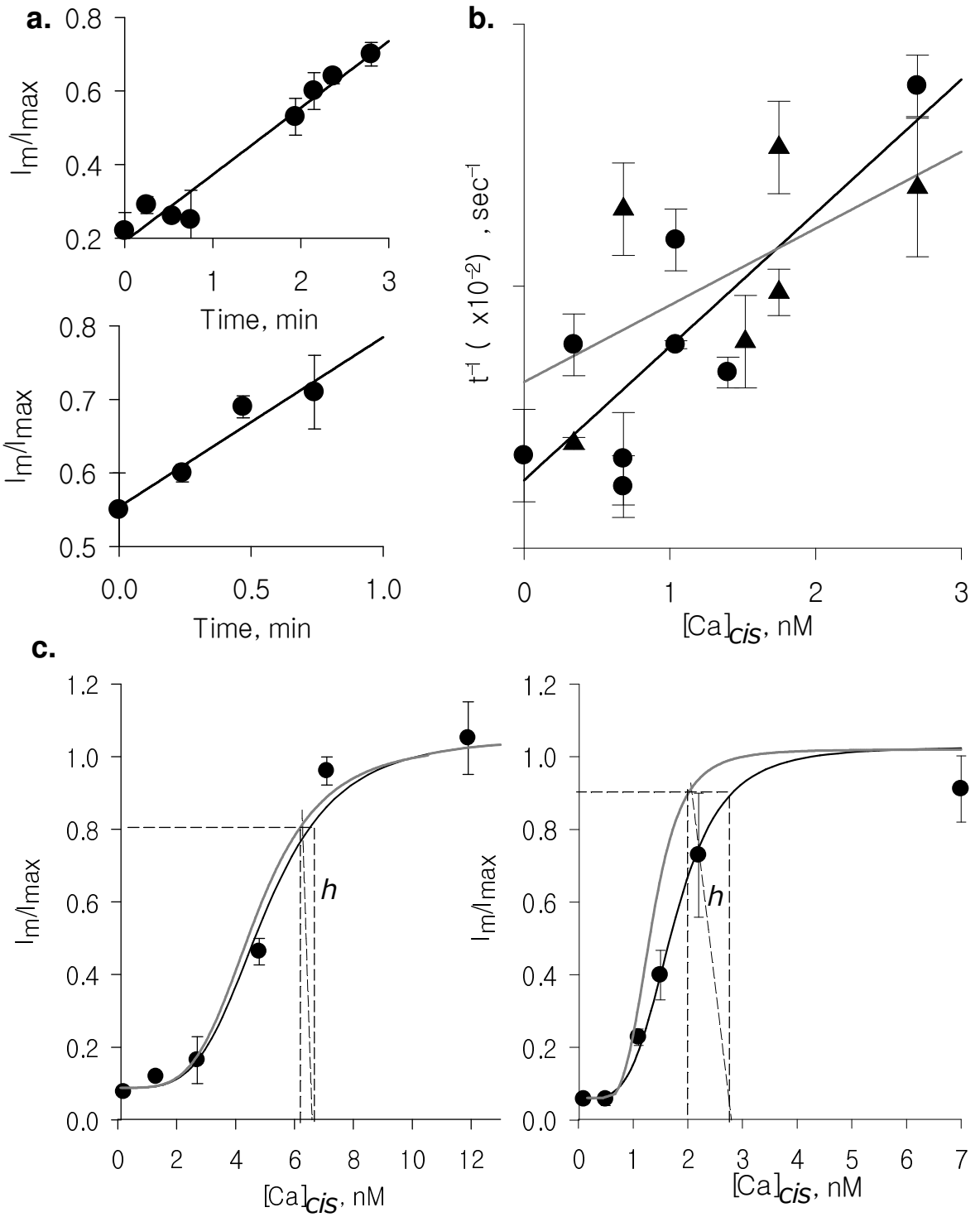

Fig. S1. ***Diffusional contribution to the K_D constants. a.*** *Representative I_m / I_{max} as a function of a given cis Ca^{2+}, after inhibition with either EGTA (upper panel, N = 4) or BAPTA (lower panel, N = 3). The solid lines represent the best fitted linear correlation. Experimental data (circles) are expressed as mean ± SEM.* ***b.*** *The slopes obtained for several Ca^{2+} concentrations (as in* ***a.****) were plotted against [Ca^{2+}] after addition of either EGTA (circles, N = 7) or BAPTA 2 mM cis (triangles, and N = 3).* ***c.*** *The Hill type curve was corrected for the diffusive process (3) for the EGTA (Left) and BAPTA (Right) curves. Experimental data plotted are the mean ± SEM.*

Modelling of $PC2_{iv}$ under various Ca^{2+} conditions using the 2S3B energy model. The single channel currents through PC2 were fitted with a 2S3B model, representing a minimal channel model that allows multiple occupancy and saturation (4). The model included six energy parameters: three peak energies (G_{12}, G_{23} and G_{34}), two well energies (G_2 and G_3), and three electrical distances (d_1 to d_3), that represent the fraction of the electric field energetically separating peaks and wells, with the requirement that the sum $2(d_1+d_2+d_3)$ equals one. An interaction parameter, $A = F_{out}/F_{in}$, was also included to represent ion-ion interactions, where F_{in} and F_{out} are the repulsion factors inside and out the channel, respectively, whenever the channel is occupied by ions. I/V experimental data were fitted, for high activity range (4, 5) with Eq. S1:

$$I = zFQ\,exp\left(-G_{23}+G_3+G_2\right)A\left\{\frac{exp\left[\left(d_2+2d_1\right)V\right]}{\left[S^+\right]_{trans}}-\frac{exp\left[-\left(d_2+2d_3\right)V\right]}{\left[S^+\right]_{cis}}\right\} \qquad \text{Eq. (S1)}$$

where d_1, d_2 and d_3 are the electrical distances, G_{23}, G_3 and G_2 are the energy of peak and valleys respectively.

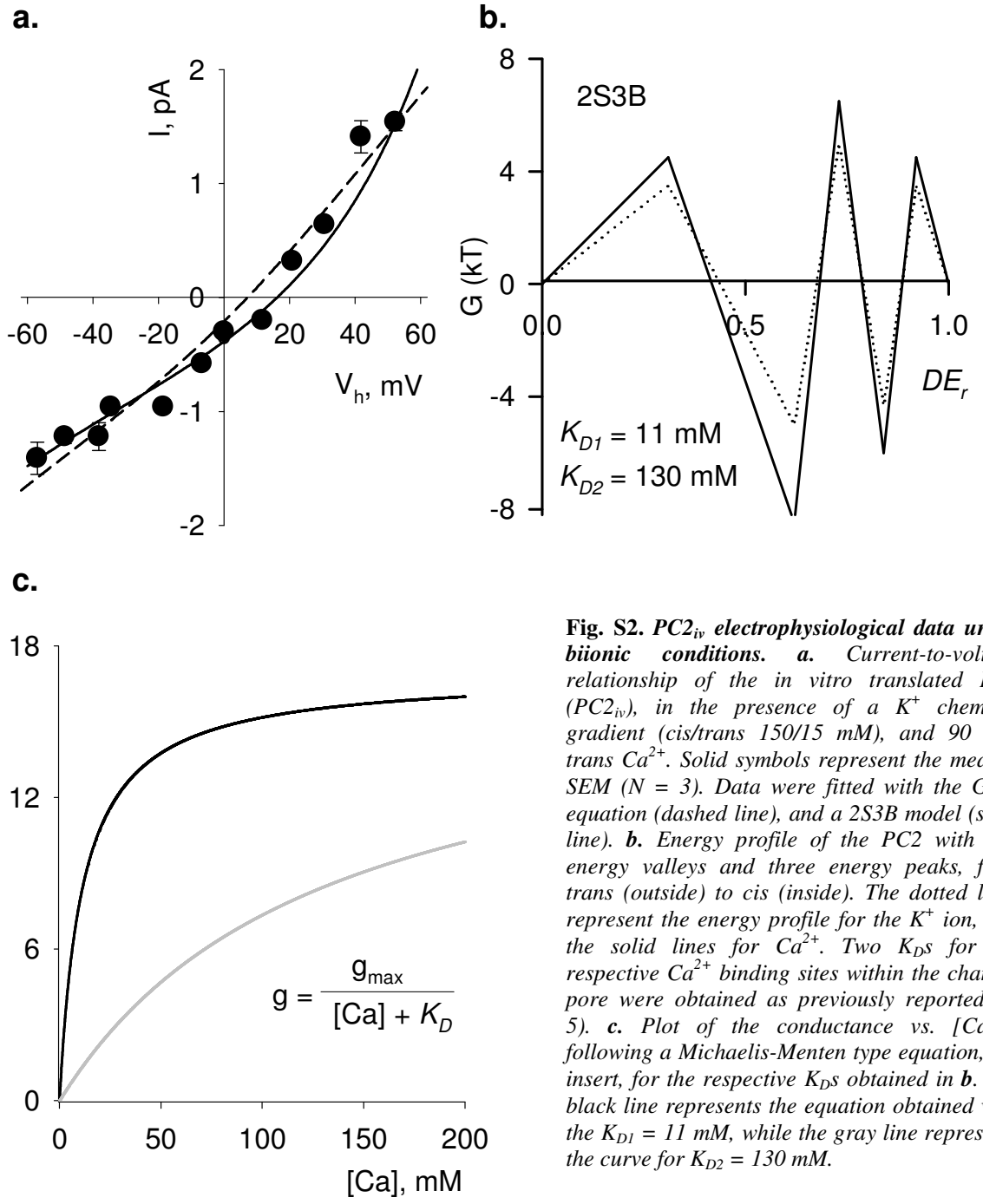

Fig. S2. ***PC2$_{iv}$ electrophysiological data under biionic conditions.*** ***a.*** *Current-to-voltage relationship of the in vitro translated PC2 (PC2$_{iv}$), in the presence of a K^+ chemical gradient (cis/trans 150/15 mM), and 90 mM trans Ca^{2+}. Solid symbols represent the mean ± SEM (N = 3). Data were fitted with the GHK equation (dashed line), and a 2S3B model (solid line).* ***b.*** *Energy profile of the PC2 with two energy valleys and three energy peaks, from trans (outside) to cis (inside). The dotted lines represent the energy profile for the K^+ ion, and the solid lines for Ca^{2+}. Two K_Ds for the respective Ca^{2+} binding sites within the channel pore were obtained as previously reported (4, 5).* ***c.*** *Plot of the conductance vs. [Ca^{2+}], following a Michaelis-Menten type equation, see insert, for the respective K_Ds obtained in* ***b****. The black line represents the equation obtained with the K_{D1} = 11 mM, while the gray line represents the curve for K_{D2} = 130 mM.*

Table S1. *NP_o obtained for $PC2_{iv}$ under various Ca^{2+} gradients*

Condition $[Ca^{2+}]_{cis}/[Ca^{2+}]_{trans}$	NP_o	SE (N = 3)
10 μM / 10 μM*	0.93	0.01
0.6 nM / 0.6 nM	0.94	0.02
0.6 nM / 10 μM	0.94	0.04
0.6 nM / 50 mM	0.90	0.04

*Control condition

Table S1 Legend. The Table summarizes the NP_o obtained for the $PC2_{iv}$ protein under various Ca^{2+} gradients showing the lack of response to high Ca^{2+} in the *trans* compartment.

Table S2. *Affinity factors of expanded Hill equation*.

	EGTA	**BAPTA**
K_S, *nM*	111.6 ± 6.92	105.0 ± 6.35
a	0.1190 ± 0.0024	0.0421 ± 0.0004
b	0.1289 ± 0.0089	0.0689 ± 0.0054
c	0.1603 ± 0.0205	0.2095 ± 0.0323
K_D ($= a^3b^2cK_s^4$), *nM*	5.14	1.73

Table S2 Legend. The Table summarizes the affinity factors obtained with Eq. (3) from dose-response recovery curves after inhibition with either EGTA (N = 7), or BAPTA (N = 5).

Table S3. *Phenomenological model parameters.*

Ca_{trans}	EGTA				
	A	*B*	*C*	*D*	*r*
0.6 nM	1.00 ± 0.08	-0.11 ± 0.08	1.05 ± 0.18	0.55 ± 0.07	0.93 ± 0.10
10 μM	1.00 ± 0.13	-0.15 ± 0.02	-0.36 ± 0.10	1.12 ± 0.55	0.96 ± 0.10
1 mM	1.00 ± 0.17	0.03 ± 0.06	0.45 ± 0.43	0.57 ± 0.45	0.55 ± 0.30
	BAPTA				
	A	*B*	*C*	*D*	*r*
10 μM	1.00 ± 0.05	-0.11 ± 0.01	1.16 ± 0.13	0.53 ± 0.04	0.97 ± 0.07
1 mM	1.00 ± 0.05	0.01 ± 0.02	2.65 ± 1.20	4.19 ± 1.15	0.82 ± 0.05

Table S3 Legend. The Table summarizes the parameters obtained from fitting the phenomenological model equation to experimental data under the various conditions indicated in the Table. Parameters *B*, *C*, and *D* are expressed in min^{-1}, while parameter *A* and regression coefficient "*r*" are dimensionless.

Supporting References

1. González-Perrett, S., K. Kim, C. Ibarra, A. E. Damiano, E. Zotta, M. Batelli, P. C. Harris, I. L. Reisin, M. A. Arnaout, and H. F. Cantiello. 2001. Polycystin-2, the protein mutated in autosomal dominant polycystic kidney disease (ADPKD), is a Ca^{2+}-permeable nonselective cation channel. Proc. Natl. Acad. Sci. USA 98:1182-1187.

2. Naraghi, M., and E. Neher. 1997. Linearized buffered Ca^{2+} diffusion in microdomains and its implications for calculation of $[Ca^{2+}]$ at the mouth of a calcium channel. J. Neurosci. 17:6961-6973.

3. Bisswanger, H. 2008. *Enzyme Kinetics. Principles and Methods*. 2nd Ed. Wiley-VCH, Weinheim.

4. Hille, B., and W. Schwarz. 1978. Potassium channels as multi-ion single-file pores. J. Gen. Physiol. 72:409-442.

5. Cantero, M. R., and H. F. Cantiello. 2011. Effect of lithium on the electrical properties of polycystin-2 (TRPP2). Eur. Biophys. J. 40:1029-1042.